NJC

Accepted Manuscript

Journal Name

ARTICLE

"Not Quenched" Aggregates of Triphenylene Derivative for the Sensitive Detection of Trinitrotoluene in Aqueous Medium

Harshveer Arora, Subhamay Pramanik, Manoj Kumar, and Vandana Bhalla*

Triphenylene derivative **4** bearing gallic acid groups at the periphery has been synthesized. Derivative **4** formed "not quenched" porous aggregates in mixed aqueous medium. These aggregates served as potent chemosensor for selective detection of trinitrotoluene (TNT) in mixed aqueous media and the detection limit in the range of 228.6×10^{-12} g/L (228.6 parts per quadrillion) was observed. Interestingly, due to porous morphology of these aggregates of derivative **4** could detect TNT in vapor phase also. In addition, the dip strips coated by the aggregates of derivative **4** could detect TNT in contact mode with detection limits of 22.7 attograms/cm^2.

Introduction:

Among various nitroaromatic compounds (NACs), 2,4,6-trinitrotoluene (TNT) is widely used in explosive materials and is a constituent of unexploded landmines worldwide.[1] Beside this, TNT is considered as potent environmental pollutant and threat to human health.[2] Trinitrotoluene is carcinogenic[3] and its continuous exposure results in headache, skin irritation, anaemia, abnormal liver function[4] and it can contaminate the ground water of war zone, thus, posing a serious threat to the environment.[5] This necessitates the development of new approaches for trace detection of TNT in aqueous media. Till date several techniques have been developed for the detection of TNT such as ion mobility spectroscopy (IMS),[6] gas chromatography mass spectroscopy (GC-MS),[7] plasma desorption mass spectrometry (PDMS),[8] energy dispersive X-ray diffraction (EDXRD),[9] surface enhanced Raman spectroscopy (SERS),[10] tetrahertz spectroscopy,[11] however, these techniques are costly, complicated and time consuming which limits their application for on-site analysis. On the other hand, fluorescence based method for detection of TNT has attracted a lot of research interest due to its high sensitivity, low cost, real time monitoring with fast response time.[12] In this context, a variety of fluorescent nanofibres[13a-b], conjugated polymers[13c-n], metal-organic frameworks[14a-b] and graphene nano-sheets[14c-d] for efficient detection of TNT[15] have been developed.

Recently, several electron rich fluorescent materials based on polycyclic aromatic hydrocarbons (PAHs) also have been developed for sensitive detection of TNT.[16] Among various PAHs, triphenylene and its derivatives are known for their unique optical properties, charge transfer mobility's and

thermal stability.[17] Though there are several reports regarding utilization of triphenylene derivatives for detection of 2,4,6-trinitrotoluene (TNT), 2,4-dinitrotoluene (DNT), and picric acid (PA) in organic media[18] yet to the best of our knowledge, there is no report regarding utilization of triphenylene derivative for the detection of TNT in aqueous media. The major problem for utilization of triphenylene derivatives for detection of nitroaromatics in aqueous media is their tendency to undergo self-assembly to form non-luminescent H-aggregates through π-π intermolecular stacking of triphenylene molecules.[19] Thus, development of fluorescent assemblies of triphenylene derivatives for the detection of nitroaromatic explosive in aqueous media is still a challenge.

Our research work involves the development of fluorescent assemblies for the detection of nitroaromatics in aqueous media and vapour phase.[20] In continuation of this work and keeping in mind the highly electron rich nature of triphenylene derivatives, we were then interested in synthesis of triphenylene derivative which could undergo self-assembly to form "not quenched" aggregates and for this purpose, we have designed and synthesized triphenylene derivative **4** having gallic acid groups at the periphery connected *via* amide groups. We envisioned that π-π intermolecular stacking between triphenylene derivatives supported by hydrogen bonding between amide groups will generate aggregates of derivative **4** in mixed aqueous media. We further expected that presence of alkyl chains will prevent the face to face packing of molecules[21] and will assist in the formation of fluorescent aggregates of derivative **4**. Interestingly, derivative **4** formed π-π stacked units which are interconnected through hydrogen bonds in slipped fashion to form a closely packed fluorescent supramolecular polymer in mixed aqueous media. Further, these aggregates could detect TNT with a detection limit in the range of 228.6 ppq or 228.6×10^{-12} g/L and the system was found to be more sensitive towards TNT in comparison to DNT and PA. Further, the solution coated test

a. *Department of Chemistry, UGC Sponsored Centre for Advanced Studies-II, Guru Nanak Dev University, Amritsar-143005, Punjab, India.*
E-mail: vanmanan@yahoo.co.in.

strips of aggregates of derivative **4** can detect TNT in the attogram range, thus, providing a low cost, portable and onsite detection method of TNT. To the best of our knowledge, this is first report of formation of 'not quenched' aggregates of triphenylene derivative in aqueous media and their utilization for detection of TNT in solution and vapour phase. Further, fluorescent supramolecular aggregates of derivative **4** exhibited more sensitive response towards TNT as compared to the other systems reported in the literature (Table S1, ESI†).

Results and discussion

Synthetic procedures and characterization

Alkylated gallic acid **1**[22] and triphenylene derivative **3**[23] were synthesized by reported methods. Further, reaction of alkylated gallic acid with $SOCl_2$ yielded alkylated gallic acid chloride, **2** which on condensation with triphenylene hexamine **3** in dry THF under nitrogen atmosphere at $0°C$ furnished derivative **4** in 60% yield (Scheme 1). The structure of compound **4** was confirmed from its spectroscopic and analytical data. The ^1H NMR spectrum of compound **4** showed five signals at δ 0.90 (CH_3, 54H), 1.25-1.34 (CH_3-CH_2, 36H), 1.49-1.56 (72H), 1.74-1.82 (36H, OCH_2-CH_2) and triplet at 4.02 (OCH_2, 36H) corresponding to the aliphatic protons, four signals at 7.07 (6H, ArH), 7.36 (12H, ArH), 7.58 (12H, ArH), 7.78 (6H, ArH), 8.70 (6H, ArH) and a signal at 3.48 (6H, NH) corresponding to the aromatic and amide protons respectively (Fig. S11, ESI†). The structure of derivative **4** was further confirmed from MALDI-TOF mass spectroscopy which showed a peak at 3222.6223 $[M+Na]^+$ (Fig. S13, ESI†). Further the FT-IR spectrum of derivative **4** showed a peak at 1648 cm^{-1} corresponding to carbonyl group stretching and a broad peak at 3431 correspond to NH amide stretching which confirms the presence of amide bond in derivative **4** (Fig. S14, ESI†). These spectroscopic results corroborate the structure **4** for this compound.

(i) $SOCl_2$, Reflux

(ii) THF, TEA, N_2, $0°C$ to RT
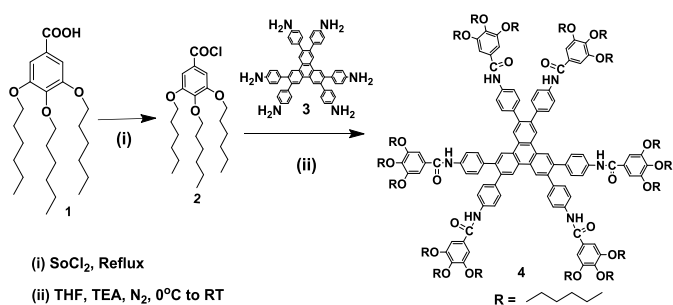
Scheme 1: Synthesis of triphenylene based derivative **4**.

Photophysical behaviour

The UV-vis spectrum of derivative **4** in THF shows an absorption band at 319 nm (Fig. 1A). Upon addition of water fraction from 0 to 60% volume in THF solution of derivative **4**, broadening of absorption signal along with a bathochromic shift of 11 nm from 319 to 330 nm was observed (Inset, Fig. 1A(ii)) Additionally, the 'levelling off tail' was observed in the

visible region of spectrum which indicates the formation of aggregates of derivative **4**. The fluorescence spectrum of derivative **4** exhibits a broad emission band at 417 nm when excited at 319 nm. The fluorescence spectra show the decrease in emission intensity with increasing water fraction from 0 to 60% (Fig. 1B), whereas, upon addition of water fraction above 60% to 90%, an abrupt increase in emission intensity was observed (Inset, Fig. 1B(iii)). These results clearly indicate the formation of 'not quenched' aggregates of derivative **4**.[20e] The dynamic light scattering (DLS) studies clearly showed average size around 396 nm, 190 nm, 141 nm and 91 nm in 30%, 50%, 70%, and 90% H_2O:THF solvent mixture of derivative **4**, respectively (Fig. S1-S2, ESI†). We assume that as the particles tend to shrink in size with increasing water content in the solvent mixture, a more coplanar conformer imposed by the congested environment in the shrunk particles is responsible for this emission enhancement.[24] Further, the scanning electron microscopic (SEM) image of derivative **4** shows the presence of porous aggregates in H_2O:THF (9:1) medium (Fig. 2A). The polarized optical microscope (POM) image of well dried aggregates of derivative **4** shows star shaped texture upon cooling which suggest the formation of ordered aggregates in H_2O:THF mixture (Fig. 2B). Further, we carried out concentration dependent ^1H NMR studies of derivative **4** in DMSO-d_6. With increasing concentration of compound **4**, downfield shifting of amide protons was observed which suggest that the amide NH groups are involved in the formation of intermolecular hydrogen bonding within the aggregates. Furthermore, upfield shifting of all aromatic protons was observed (Fig. 3) which is attributed to the intermolecular shielding from the neighbouring aromatic molecules in the concentrated solution indicating the π-π stacking of derivative **4** upon increasing the
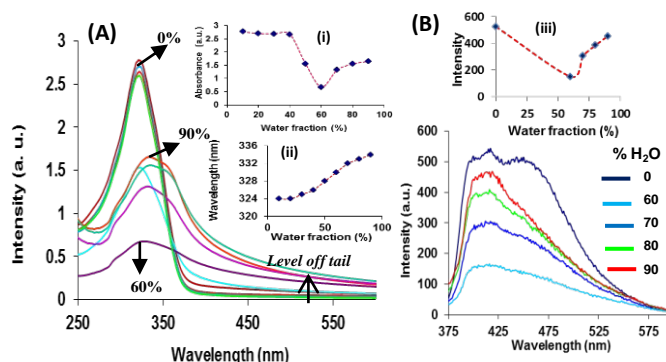

Fig. 1: (A) UV-vis spectrum of derivative **4** (15 µM) in different fractions of water in THF, inset showing (i) Variation in absorbance with different water fractions; (ii) Bathochromic shift of emission with increasing water fractions in THF; (B) Fluorescence spectrum of derivative **4** (10 µM) in different fractions of water in THF; Inset showing (iii) the variation in emission intensity with the change in water fractions.

concentration.[25a-c] On the basis of all these studies, we propose that upon self-assembly, the molecules of derivative **4** form π-π stacked units which are interconnected through hydrogen bonds in slipped fashion to form a closely packed fluorescent supramolecular aggregates.[24] We believe that dense packing of molecules of derivative **4** in aggregated state, formation of coplanar nano-sized aggregates in aqueous media

and restriction to the intramolecular rotation of the rotors attached to the triphenylene core are the main reasons for the formation of fluorescent aggregates in case of derivative **4**.[25d]
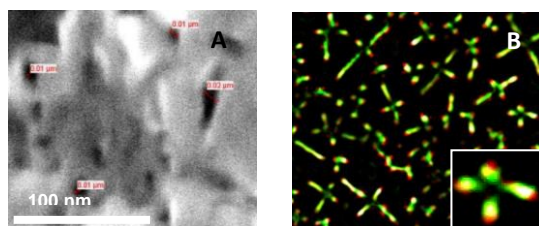
Fig. 2: (A) Scanning Electron microscope (SEM) image of derivative **4** in H₂O:THF (9:1); magnification = 100 nm **(B)** Polarized optical microscope (POM) image of aggregates of derivative **4** at room temperature after cooling from 350°C. Inset shows a magnified texture.
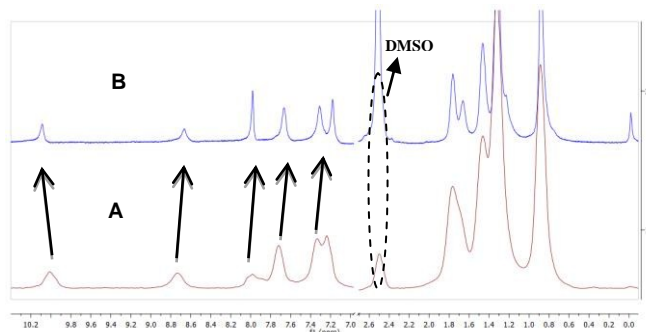
Fig. 3: ^{1}H NMR spectrum of derivative **4** upon increasing the concentration from (A) 2 mg/0.6ml to (B) 5 mg/0.6 ml in DMSO-d₆.

Detection of TNT

Further, the high emission intensity of derivative **4** in H₂O:THF (9:1) mixture (Φ=0.4)[26] prompted us to explore potential application of these aggregates as chemosensor for detection of nitro derivatives such as 2,4,6-trinitrotoluene (TNT), 2,4,6-trinitrophenol (TNP/PA), 2,4-dinitrotoluene (DNT), 1,4-di-nitrobenzene (DNB), 4-nitrotoluene (NT), 2,4-dinitrophenol (DNP), nitromethane (NM), 2,3-dimethyl-2,3-dinitrobutane (DMNB) and electron deficient 1,4-benzoquinone (BQ). The emission of derivative **4** in H₂O:THF (9:1) mixture was completely quenched upon the addition of 0.15 equiv. of TNT (Fig. 4A). This quenching of fluorescence was clearly visible to naked eye when observed under the UV light of 365 nm (Inset Fig. 4A).

Fluoremetric detection of TNT

The quenching of fluorescence with TNT was studied by Stern-Volmer relationship (Fig. 4B). The Stern-Volmer plot of derivative **4** was found to be hyperbolic curved which was straight line at lower concentration (upto 0.6 µM, Inset Fig. 4B) with Stern-Volmer constant of 13.33×10^5 M^{-1} but at higher concentration it bends upwards due to superamplified quenching effect.[27] This is attributed to the 3-dimensional topological structures of the aggregates of derivative **4** that generate more small cavities or pores, which offer more diffusion channels for the excitons to migrate, thus, allowing them to be more quickly annihilated by the explosive quenchers.[28] The detection limit of aggregates of derivative **4** for TNT was found to be 228.6 ppq (1.007×10^{-12} mol/L or

228.6×10^{-12} g/L) (Fig. S3, ESI†) which is much below the maximum limit for TNT in drinking water as set by US EPA. The calculated limit of detection (LOD) is also very low in comparison to other reported chemosensors for TNT (Table S1, ESI†). The negligible spectral overlap between absorption spectrum of TNT and emission spectrum of derivative **4** (Fig. S4 ESI†) eliminate the possibility of energy transfer event for the observed fluorescence quenching. Further, the absorption spectrum of derivative **4** showed a decrease in levelling of tail upon the addition of TNT (Fig. S5A, ESI†).[28]
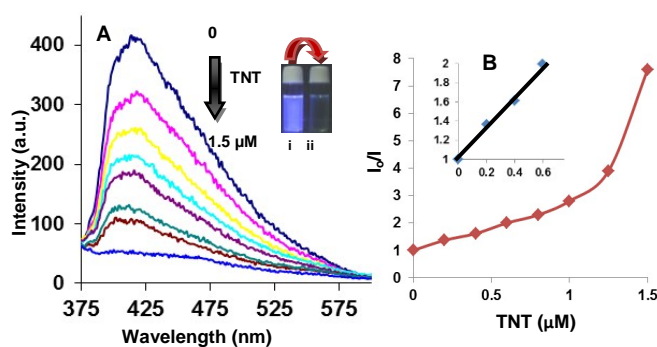
Fig. 4: (A) Fluorescence spectrum of derivative **4** (10 µM) upon the addition of 2,4,6-trinitrotoluene (TNT) from 0 to 1.5 µM in H₂O:THF (9:1) mixture. Inset shows the fluorescence of derivative **4** under UV light of 365 nm (i) before and (ii) after the addition of TNT. **(B)** Stern-Volmer plot for the quenching of derivative **4** with TNT. Inset shows the Stern-Volmer plot at low concentration (upto 0.6 µM).

Mechanism for the detection of TNT

Further, we carried out time resolved fluorescence studies of aggregates of derivative **4** in the excited state in the presence and absence of TNT in H₂O:THF (9:1) mixture (Fig. 5). Derivative **4** showed lifetime of 4×10^{-12} sec in the absence of TNT. Further, the life time is decreased (0.658×10^{-12} sec) upon addition of TNT (0 to 1.5 µM) which shows that quenching is dynamic in nature. Further, plot of change of decay time *vs* concentration of TNT is hyperbolic curve (Fig. 5B) which supports the dynamic nature of fluorescence quenching due to the charge transfer from derivative **4** to electron deficient TNT.[29] To get insight into the mechanism of sensing of TNT, we also carried out the ^{1}H NMR studies of derivative **4** in DMSO-d₆:D₂O (8:2) solution in presence of TNT. Upon the addition of TNT, all the signals get broadened and show slight upfield shift of 0.06 ppm was observed (Fig. S6, ESI†). To rule out the effect of solvent, we also carried out fluorescence spectra of derivative **4** in H₂O:DMSO (9:1, v/v) in presence of TNT (0 to 1.6 µM) and almost similar results was obtained as in case of THF/H₂O mixture (Fig. S5B, ESI†). These studies confirm charge transfer mechanism in which aggregates of **4** acts as a donor and TNT as acceptor. The charge transfer mechanism was supported by cyclic voltammetric studies (Fig. S7, ESI†). The HOMO energy level of derivative **4** was found to be -5.84 eV by taking -4.8 eV as HOMO of ferrocene/ferrocenium redox system. Further, from band gap (calculated from absorption spectrum), the LUMO energy level of derivative **4** was found to be -2.54 eV. The higher value of LUMO of derivative **4**

facilitates the jump of electron to lower lying LUMO of TNT (LUMO = -3.78 eV).[30]

Selective detection of TNT

We also carried out the fluorescence studies of derivative **4** with TNT in THF and only 35% quenching was observed upon the addition of 1.5 µM of TNT (Fig. S8, ESI†). We believe that, porous morphology of aggregates of derivative **4** enable the small explosive TNT molecules to enter through charge transfer interactions and offer more diffusion channels for the excitons to migrate, allowing them to be more quickly annihilated by the explosive quenchers (Fig. S9, ESI†).[27, 31] Under the similar set of conditions, we have also tested fluorescence response with other nitroaromatic compounds. The quenching was also observed with DNT (56%), PA (25%), DNB (20%) 4-NT (10%), DNP (5%), NP (3%) upon the addition of 1.5 µM of these NACs (Fig. 6). However, in case of nitro derivatives (NB, DMNB and NM) and electron deficient compounds (BQ and BA) negligible quenching was observed. Thus, aggregates of derivative **4** exhibit more sensitive response towards TNT as compared to other nitroaromatics.
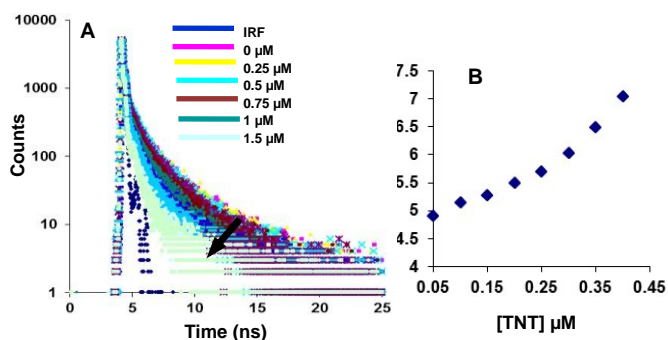

Fig. 5 (A) Time resolved fluorescence spectrum of derivative **4** (10 µM) upon increasing the concentration of TNT from 0 µM to 1.5 µM (B) Stern-Volmer plot for decay time of derivative **4** *vs.* concentration of TNT
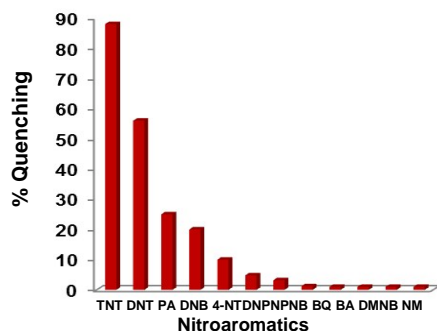

Fig. 6: Bar diagram showing the percentage quenching of florescence of derivative **4** (10 µM) with various nitroaromatic compounds (1.5 µM) in H_2O:THF (9:1) mixture.

Vapour phase detection of TNT

Till date there are very few reports about the utilization of chemosensors for detection of TNT in vapour phase.[13b] The porous morphology of the supramolecular aggregates of derivative **4** prompted us to examine their sensing ability for detection of TNT in vapour phase. For the vapour phase detection of TNT, we exposed the aggregates of derivative **4** in H_2O:THF (9:1) mixture to the vapors of TNT by placing the vial containing solution in the big vial containing solid TNT at base and then fluorescence spectrum of this solution was recorded

after particular time interval. Aggregates of derivative **4** showed 10% quenching of fluorescence within the 2 minutes of exposure to TNT vapours however, further exposure to TNT vapours upto 6 minutes resulted in 16% quenching of fluorescence (Fig. S10, ESI†). Thus, aggregates of derivative **4** can detect TNT in aqueous medium and in vapour phase.
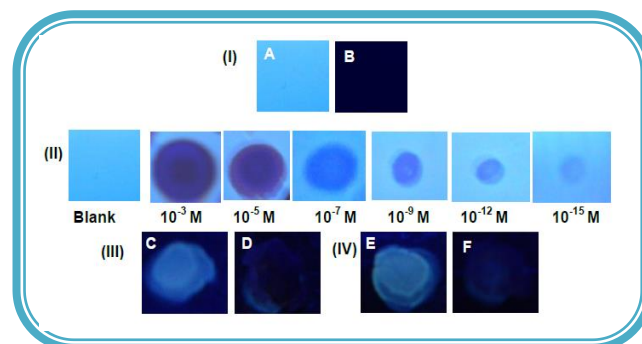

Fig. 7: Fluorescent test strips of derivative **4** for the detection of TNT. **(I)** A) Test strip B) Test strip dipped in 10^{-5} M solution of TNT **(II)** Test strips with different concentrations of TNT (10^{-3} to 10^{-15} M); **(III)** c) Thin film of derivative **4** on glass slide and D) after adding one drop of TNT solution (10^{-5} M in THF) **(IV)** Vapor phase sensing of TNT with thin film of derivative **4**

Practical application for the TNT detection through paper strip

Further, preparation and packing of explosives is often accompanied by contamination of human body, clothes and surroundings.[32] Therefore, to detect trace amounts of TNT, we have prepared the solution coated test strips of derivative **4** by dipping them in the solution of derivative **4** in H_2O:THF (9:1) mixture followed by drying it under vacuum. The test strip when dipped in 10^{-5} M solution of TNT showed complete quenching of fluorescence (Fig. 7; I). To detect the trace amounts of TNT, 10 µl of TNT solutions of different concentrations were poured over the solution coated test strips covering the ~0.1 cm^2, the dark spots of different intensities were formed (Fig. 7; II) which showed the regulation of intensities of spots with the concentration of analyte. The minimum concentration of TNT which can be detected with naked eye was up to 10^{-15} M which corresponds to 22.7 ag cm^{-2} which is lower than the other reported system for detection of TNT in the literature.[16d] Further, the thin film of derivative **4** formed by drop casting method on glass slide also showed instant quenching upon addition of a drop of TNT solution on it (Fig. 7; III). The vapour phase sensing of TNT was performed in solid state by exposing the thin film of derivative **4** on glass slide to the vapours of TNT by placing it over the vial containing solid TNT for 6 minutes. The film showed quenching of fluorescence under the UV light of 365 nm (Fig. 7; IV). Although a variety of fluorescent materials have been reported for the detection of TNT, but most of these materials suffer from several limitations such as poor detection limit, interference from other nitroaromatics especially DNT and most of these materials could detect TNT only in solution and solid phase. Furthermore, in case of polymeric materials, their multi step conventional covalent synthesis limit their real time monitoring of TNT. In comparison, the probe being reported in this present manuscript could detect TNT in solid, liquid and

vapour phases with very low detection limit and give selective response towards TNT over DNT and PA (Table S1, ESI†).

Conclusions

In conclusion, we designed and synthesized gallic acid substituted extended triphenylene derivative **4** having amide linkages. The derivative **4** formed porous aggregates in H_2O:THF (9:1) mixture. Among the various nitroaromatic explosives tested, these aggregates serve as potent chemosensor for picomolar detection of 2,4,6-trinitrotoluene (TNT) in aqueous medium and in vapour phase. The practical application of derivative **4** as TNT chemosensor was realized by making the solution coated test strip and thin films on glass which could detect TNT in solution and vapour phase, respectively.

Experimental

Synthesis of Derivative 4

To the solution of **1** (440 mg, 1.04 mmol) in dry DCM (10 ml) was added freshly distilled $SOCl_2$ (5 ml) dropwise, under N_2 at room temperature. After the addition, the reaction was stirred at room temperature for 12 hrs. After that, thionyl chloride was removed and residue was dried under vacuum. The solution of this crude compound **2** (409 mg, 0.930 mmol) in dry THF (5 ml) was added dropwise to the ice cold solution of derivative 3 (100 mg, 0.13 mmol) in dry THF (5 ml) in the presence of triethylamine (0.093 ml) under N_2 atmosphere. The resulting mixture was stirred at room temperature for 24 hrs. After the completion of reaction, the reaction mixture was diluted with chloroform (25 ml) and washed with water (2×20 ml), the organic layer was dried over Na_2SO_4, concentrated under vacuum to get crude product which was purified by column chromatography ($CHCl_3$:Hex. 2:8) to give compound **4** in 60% yield. ^{1}H NMR (500 MHz, $CDCl_3$, ppm): δ = 0.90 (s, CH_3, 54H), 1.25-1.34 (m, CH_3-CH_2, 36H), 1.49-1.56 (m, 72H), 1.74-1.82 (m, OCH_2-CH_2, 36H), 3.48 (s, 6H, NH) 4.02 (t, OCH_2, J = 5.0 Hz, 36H), 7.07 (s, 6H, ArH), 7.36 (d, J = 5.0 Hz, 12H, ArH), 7.58 (d, J = 5.0 Hz, 12H, ArH), 7.78 (s, 6H, ArH), 8.70 (s, 6H, ArH). ^{13}C NMR (125 MHz, $CDCl_3$, ppm): δ = 14.20, 22.58, 25.77, 29.34, 30.24, 31.51, 69.00, 73.13, 106.47, 120.67, 125.60, 128.67, 129.99, 130.37, 136.73, 138.26, 139.73, 139.81, 140.60, 152.71, 165.71. MALDI-TOF MS m/z: 3222.6223 $[M+Na]^+$. Elemental analysis: Calculated for: $C_{204}H_{282}N_6O_{24}$: C, 76.51; H, 8.88; N, 2.62; Found: C, 76.49 H, 8.81; N, 2.57. The FT-IR showed stretching bands at 3431, 2858 and 1648 cm^{-1} corresponding to NH, O-CH_2 and C=O groups. These spectroscopic results corroborate the structure **4** for this compound (Fig. S11-S14, ESI†).

General Experimental Methods and Materials

All reagents were purchased from Aldrich and were used without further purification. THF was dried over sodium and benzophenone as an indicator. UV-vis studies were performed in THF, distilled water and HEPES buffer (pH=7.05).

All the UV-Vis spectra were recorded on SHIMADZU UV-2450 spectrophotometer. All the fluorescence spectra were recorded on SHIMADZU RF 5301 PC spectrofluorometer. ^{1}H and ^{13}C NMR spectra were recorded on JEOL-FT NMR-AL 300 MHz and BRUKER-AVANCE-II FT-NMR-AL 500 MHz spectrophotometer using $CDCl_3$ as solvent and TMS as internal standards. Data are reported as follows: chemical shifts in ppm (δ), multiplicity (s = singlet, d = doublet, br = broad singlet, m = multiplet), coupling constants (Hz), integration, and interpretation. SEM images were obtained with a field emission scanning electron microscope (SEM CARL ZEISS SUPRA 55). Polarized optical microscopic (POM) images were recorded on a NIKON ECLIPSE LV100 POL. Time resolved fluorescence studies were performed on Horriba Time Resolved Fluorescence Spectrometer instrument using time correlated single photon counting (TPSPC) technique. The dynamic light scattering (DLS) data was recorded using Zetasizer Nano, ZS Malvern Instrument Ltd., U.K.

Quantum yield calculations

Fluorescence quantum yield was determined by using optically matching solution of diphenyl anthracene (Φ_{fr} = 0.90 in cyclohexane) as standard at an excitation wavelength of 373 nm and quantum yield is calculated using the equation:

$$\Phi_{fs} = \Phi_{fr} \times \frac{1-10^{-A_rL_r}}{1-10^{-A_sL_s}} \times \frac{N_s^2}{N_r^2} \times \frac{D_s}{D_r}$$

Φ_{fs} and Φ_{fr} are the radiative quantum yields of sample and the reference respectively, A_s and A_r are the absorbance of the sample and the reference respectively, D_s and D_r the respective areas of emission for sample and reference. L_s and L_r are the lengths of the absorption cells of sample and reference respectively. N_s and N_r are the refractive indices of the sample and reference solutions (pure solvents were assumed respectively).

Calculation of Stern-Volmer constants

The sensitivity of derivative **4** towards the nitroaromatic compounds was estimated from their Stern-Volmer constants K_{sv} as determined from equation

$$I_o/I = 1+K_{sv}\,[Q]$$

Where I_o and I are the fluorescence intensities in the absence and in the presence of nitroaromatics respectively and Stern-Volmer plots were plotted as a function of nitroaromatic concentration [Q]. The Stern-Volmer constants, K_{sv} can be calculated from the slope of Stern-Volmer plots.

UV-vis and fluorescence titrations

UV-vis and fluorescence titrations were performed on 10.0 μM solutions of ligand **4** in H_2O:THF (9:1, v/v). Typically, aliquots of freshly prepared standard solutions (10^{-1} M to 10^{-3} M) various nitro derivatives are examined such as 2,4,6-trinitrotoluene (TNT), 2,4,6-trinitrophenol (TNP/PA), 2,4-dinitrotoluene (DNT), 1,4-di-nitrobenzene (DNB), 4-nitrotoluene (NT), 2,4-dinitrophenol (DNP), nitromethane (NM), 2,3-dimethyl-2,3-dinitrobutane (DMNB) and electron deficient 1,4-benzoquinone (BQ). In titration experiments, each time a 3 ml solution of compound was filled in a quartz cuvette (path length, 1 cm) and spectra were recorded.

Experimental details for detection of TNT

Preparation of test strips

Test strips for solid state detection of TNT were prepared by coating the solution of derivatives **4** (10^{-3} M) on Whatman filter paper followed by the removal of solvent under vacuum. These filter paper was then cut into 1cm×1cm dimensions, which were used as test strips for various concentration of TNT sensing.

^{1}H NMR titrations

For NMR titrations, stock solution (600 µl of 10^{-2} M) of derivative 4 was prepared in DMSO-d_6:D_2O (8:2, v/v). Similarly, the stock solution of TNT (10 µl of 10^{-2} M) was prepared in DMSO-d_6.

Quantitative Detection of TNT by Test strip

The required TNT solution (10 µl) of various concentrations (10^{-3} to 10^{-15} M) in H_2O:THF (9:1, v/v) were added level using a glass micro-syringe over ~0.1 cm^2 area to each strip and then the solvent was allowed to evaporate. Then the fluorescence was measured under 365 nm UV lamp.

Contact Mode Detection of TNT

Thin film of compound 4 was coated on a TLC plate and dried under vacuum. Then solid TNT was put over the thin film and quenching of fluorescence was measured under 365 nm UV lamp.

Experimental details of vapour phase sensing

For the vapour phase detection of nitroaromatic explosives, the glass vial containing 3 ml of 10 µM solution of derivative 4 in H_2O:THF (9:1, v/v) was inserted in other big vial containing 5 mg of TNT crystals at the base. The system was sealed so as to obtain saturated vapour pressure at room temperature. The fluorescent spectrum of the sample was then recorded after every five minutes. For the vapour phase detection, the solution coated glass slide with thin film was placed over the vial containing TNT for 5 minutes. The area exposed to vapours showed quenching of fluorescence which was clearly visible to naked eye.

Acknowledgements

Notes and references

1 (a) Y. Hong, J. W. Y. Lam and B. Z. Tang, *Chem. Soc. Rev.,* 2011, **40**, 5361; (b) R. A. Maureen, C & EN News 1997, March 10, 14.

2 J. Yinontrends, Anal. Chem., 2002, 21, 292.

3 Toxicological profile for 2,4,6-trinitrotoluene, U.S. Department of Health and Human Services, Public Health Service, Agency for Toxic Substances and Disease Registry

4 (a) D. Ownby, J. Belden, G. Lotufo and M. Lydy, *Chemosphere,* 2005, **58**, 1153; (b) E. Etnier, *Regul. Toxicol. Pharmacol.,* 1989, **9**, 147.

5 (a) A. Fainberg, *Science,* 1992, **255**, 1531; (b) L. A. Pinnaduwage, A. Gehl, D. L. Hedden, G. Muralidharan, T. Thundat, R. T. Lareau, T. Sulchek, L. Manning, B. Rogers, M. Jones and J. D. Adams, *Nature,* 2003, **425**, 474.

6 (a) M. Tam and H. H. Hill, *Anal. Chem.,* 2004, **76**, 2741; (b) M. Najarro, M. E. D. Morris, M. E. Staymates, R. Fletcher and G. Gillen, *Analyst,* 2012, **137**, 2614.

7 (a) N. L. Sanders, S. Kothari, G. M. Huang, G. Salazar and R. G. Cooks, *Anal. Chem.,* 2010, **82**, 5313; (b) Y. Zhang, X. X. Ma, S. C. Zhang, C. D. Yang, Z. Ouyang and X. R. Zhang, *Analyst,* 2009, **134**, 176.

8 K. Hakansson, R. V. Coorey, R. A. Zubarev, V. L. Talrose and P. Hakansson, *J. Mass Spectrom.,* 2000, **35**, 337.

9 R. D. Luggar, M. J. Farquharson, J. A. Horrocks and R. J. Lacey, *X-Ray Spectrom.,* 1998, **27**, 87.

10 D. S. Moore, *Rev. Sci. Instrum.* 2004, **24**, 2499.

11 (a) M. R. Leahy-Hoppa, M. J. X. Fitch, Zheng, L. M. Hayden and R. Osiander, *Chem. Phys. Lett.,* 2007, **434**, 227; (b) W. H. Fan, A. Burnett, P. C. Upadhya, J. Cunningham, E. H. Linfield and A. G. Davies, *Appl. Spectrosc.,* 2007, **61**, 638.

12 (a) S. Kumar, N. Venkatramaiah and S. Patil *J. Phys. Chem. C,* 2013, **117**, 7236; (b) T. Naddo, Y. Che, W. Zhang, K. Balakrishnan, X. Yang, M. Yen, J. Zhao, J. S. Moore and L. Zang, *J. Am. Chem. Soc.,* 2007, **129**, 6978; (c) S. J. Toal and W. C. Trogler, *J. Mater. Chem.,* 2006, **16**, 2871.

13 (a) C. Zhang, Y. Che, X. Yang, B. R. Bunes and L. Zang, *Chem. Commun.,* 2010, **46**, 5560; (b) M. Kumar, V. Vij, and V. Bhalla, *Langmuir,* 2012, **28**, 12417; (c) T. Naddo, Y. Che, W. Zang, K. Balakrishnan, X. Yang, M. Yen, J. Zhao, J. S. Moore and L. Zhang, *J. Am. Chem. Soc.,* 2007, **129**, 6978; (d) X. Wang, Y. Guo, D. Li, H. Chen and R.-C. Sun, *Chem. Commun.,* 2012, **48**, 5569; (e) S. Shanmugaraju, S. A. Joshi and P. S. Mukherjee, *J. Mater. Chem.,* 2011, **21**, 9130; (f) J. C. Sanchez and W. C. Trogler, *J. Mater. Chem.,* 2008, 3143; (g) D. C. Apodaca, R. B. Pernites, F. R. D. Mundo and R. C. Advincula, *Langmuir,* 2011, **27**, 6768; (h) S. W. Thomas, G. D. Joly and T. M. Swager, *Chem. Rev.,* 2007, **107**, 1339; (i) A. Narayanan, O. P. Varnavski, T. M. Swager and T. Goodson, *J. Phys. Chem. C,* 2008, **112**, 881; (j) Y. Che, X. Yang, G. Liu, C. Yu, H. Ji, J. Zuo, J. Zhao and L. Zang, *J. Am. Chem. Soc.,* 2010, **132**, 5743; (k) H.-T. Feng, J.-H. Wang and Y.-S. Zheng, *ACS Appl. Mater. Interfaces,* 2014, **6**, 20067; (l) X. Wu, H. Li, B. Xu, H. Tong and L. Wang, *Polym. Chem.,* 2014, **5**, 4521; (m) N. Venkatramaiah, A. D. G. Firmino, F. A. A. Paz and J. P. C. Tome, *Chem. Commun.,* 2014, **50**, 9683; (n) S. Pramanik, V. Bhalla and M. Kumar, *Anal. Chim. Acta,* 2013, **793**, 99.

14 (a) B. Gole, A. K. Bar and P. S. Mukherjee, *Chem. Eur. J.,* 2014, **20**, 2276; (b) K. S. Bejoymohandas, T. M. George, S. Bhattacharya, S. Natarajan and M. L. P. Reddy, *J. Mater. Chem. C,* 2014, **2**, 515; (c) W. Si, W. Lei, Z. Han, Q. Hao, Y. Zhang and M. Xia, *Sensors and Actuators B,* 2014, **199**, 154; (d) K. Zhang, L. Yang, H. Zhu, F. Ma, Z. Zhanga and S. Wang, *Analyst,* 2014, **139**, 2379.

15 (a) X. Wang, Y. Guo, D. Li and R. C. Sun, *Chem. Commun.,* 2012, **48**, 5569; (b) Y. H. Lee, H. Liu, J. Y. Lee, S. H. Kim, S. K. Kim, J. L. Sessler, Y. Kim and J. S. Kim, *Chem.–Eur. J.,* 2010, **16**, 5895.

16 (a) N. Venkatramaiah, A. D. G. Firmino, F. A. Almeida Paz and J. P. C. Tome, *Chem. Commun.,* 2014, **50**, 9683; (b) P. Beyazkilic, A. Yildirim and M. Bayindir, *ACS Appl. Mater. Interfaces,* 2014, **6**, 4997; (c) G. He, N. Yan, J. Yang, H. Wang, L. Ding, S. Yin and Y. Fang, *Macromolecules* 2011, **44**, 4759. (d) K. K. Kartha, S. S. Babu, S. Srinivasan and A. Ajayaghosh, *J. Am. Chem. Soc.,* 2012, **134**, 4834; (e) X. Yang, J. Wang, D. Su,

Q. Xia, F. Chai, C. Wang and F. Qu, *Dalton Trans.,* 2014, **43**, 10057.

17 (a) S. K. Pal, S. Setia, B.S. Avinash and S. Kumar, *Liquid Crystals*, 2013, **40**, 1769; (b) B. R. Kaafarani, *Chem. Mater.* 2011, **23**, 378; (c) S. Sergeyev, W. Pisula and Y. H. Geerts, *Chem. Soc. Rev.,* 2007, **36**, 1902; (d) S. Kumar, *Chem. Soc. Rev.,* 2006, **35**, 83.

18 (a) H. Wang, X. Xu, A. Kojtari and H. F. Ji, *J. Phys. Chem. C,* 2011, **115**, 20091; (b) Y. Z. Liao, V. Strong, Y. Wang, X. G. Li, X. Wang and R. B. Kaner, *Adv. Funct. Mater.,* 2012, **22**, 726; (c) V. Bhalla, H. Arora, H. Singh and M. Kumar, *Dalton Trans.,* 2013, **42**, 969; (d) V. Bhalla, H. Singh, M. Kumar and S. K. Prasad, *Langmuir,* 2011, **27**, 15275.

19 (a) J. B. Birks, L. G. Christophorou, *Proc. R. Soc. London, Ser. A,* 1964, **277**, 571; (b) I. B. Berlman, Handbook of Fluorescence Spectra of Aromatic Molecules, Academic Press, New York, 1965, p. 171

20 (a) V. Bhalla, S. Pramanik and M. Kumar, *Chem. Commun.,* 2013, **49**, 895; (b) S. Kaur, V. Bhalla, V. Vij and M. Kumar, *J. Mater. Chem. C,* 2014, **2**, 3936; (c) S. Kaur, A. Gupta, V. Bhalla, M. Kumar, *J. Mater. Chem. C,* 2014, **2**, 7356; (d) M. Kumar, V. Vij, V. Bhalla, *Langmuir* 2012, **28**, 12417. (e) H. Arora, V. Bhalla, M. Kumar *RSC Adv.,* 2015, **5**, 32637.

21 H. Nie, G. Sun, M. Zhang, M. Baumgarten, K. Mullen, *J. Mater. Chem.,* 2012, **22**, 2129.

22 (a) S. Maruyama, K. Sato and H. Iwahashi, *Chem. Lett.,* 2010, **39**, 714; (b) A. S. Achalkumar, U. S. Hiremath, D. S. S. Rao, S. K. Prasad and C. V. Yelamaggad, *J. Org. Chem.,* 2013, **78**, 527; (c) R. Judele, S. Laschat, A. Baro and M. Nimtz, *Tetrahedron,* 2006, **62**, 9681.

23 V. Bhalla, H. Arora, A. Dhir and M. Kumar, *Chem. Commun.*, 2012, **48**, 4722.

24 (a) S. Jang, S.G. Kim, D. Jung, H. Kwon, J. Song, S. Cho, Y. C. Ko and H. Sohn, *Bull. Korean Chem. Soc.*, 2006, **27**, 12; (b) C. Cebrián, M. Natali, D. Villa, M. Panigati, M. Mauro, G. D'Alfonso and L. De Cola, *Nanoscale*, 2015, **7**, 12000; (c) R.-H. Chien, C.-T. Lai and J.-L. Hong, *J. Phys. Chem. C*, 2011, **115**, 5958.

25 a) Y. Hamuro, S. J. Geib and A. D. Hamilton, *J. Am. Chem. Soc.,* 1997, **119**, 10587; (b) S. Xiao, M. Myers, Q. Miao, S. Sanaur, K. Pang, M. L. Steigerwald and C. Nuckolls, *Angew. Chem., Int. Ed.,* 2005, **44**, 7390; (c) W. J. Liu, Y. Zhou, Y. Ma, Y. Cao, J. Wang and J. Pei, *Org. Lett.,* 2007, **9**, 4187; (d) X. Zhang, D. Gorl, V. Stepanenko and F. Wurthner, *Angew. Chem. Int. Ed.*, 2014, **53**, 1270.

26 J. N. Deams and G. Grosby, *J. Phys. Chem.,* 1971, **75**, 991.

27 J. Liu, Y. Zhong, P. Lu, Y. Hong, J. W. Y. Lam, M. Faisal, Y. Yu, K. S. Wong and B. Z. Tang, *Polym. Chem.,* 2010, **1**, 426.

28   J. Wang, J. Mei, W. Yuan, P. Lu, A. Qin, J. Sun, Y. Ma and B. Z. Tang, *J. Mater. Chem.,* 2011, **21**, 4056.

29 D. Zhao and T. M. Swager, *Macromolecules*, 2005, **38**, 9377.

30 H. Sohn, M. J. Sailor, D. Magde and W. C. Trogler, *J. Am. Chem. Soc.*, 2003, **125**, 3821

31 (a) Z. Ding, Q. Zhao, R. Xing, X. G. Wang, J. Ding, L. Wang and Y. Han, *J. Mater. Chem. C,* 2013, **1**, 786; (b) X. Liu, X. Zhang, R. Lu, P. Xue, D. Xu and H. Zhou, *J. Mater. Chem.*, 2011, **21**, 8756.

32 (a) T. H. Kim, B. Y. Lee, J. Jaworski, K. Yokoyama, W.J. Chung, E. Wang, S. Hong, A. Majumdar and S.W. Lee, *ACS Nano,* 2011, **5**, 2824; (b) K. J. Albert, N. S. Lewis, C. L. Schauer, G. A. Sotzing, S. E. Stitzel, T. P. Vaid and D. R. Walt, *Chem. Rev.,* 2000, **100**, 2595.

Graphical Abstract
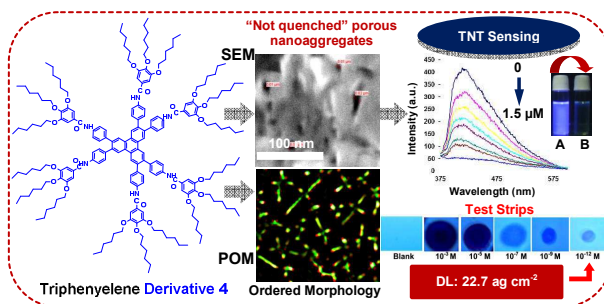
"Not quenched" porous aggregates of triphenylene derivative **4** have been utilized for detection of TNT in solution, solid and vapour phase with detection limits 22.7 attograms/cm^2.